Influence of Different Operation Conditions on Soot Formation from C 2 H 2 Pyrolysis

ARTICLE *in* INDUSTRIAL & ENGINEERING CHEMISTRY RESEARCH · NOVEMBER 2007

Impact Factor: 2.59 · DOI: 10.1021/ie070008i

5 AUTHORS, INCLUDING:

Roberto Guzman de Villoria
Madrid Institute for Advanced Studies
65 PUBLICATIONS **906** CITATIONS
SEE PROFILE

A. Millera
University of Zaragoza
67 PUBLICATIONS **898** CITATIONS
SEE PROFILE

María U. Alzueta
University of Zaragoza
116 PUBLICATIONS **1,904** CITATIONS
SEE PROFILE

Rafael Bilbao
University of Zaragoza
151 PUBLICATIONS **2,606** CITATIONS
SEE PROFILE

Influence of Different Operation Conditions on Soot Formation from C_2H_2 Pyrolysis

M. Pilar Ruiz,*,† Roberto Guzmán de Villoria,‡ Ángela Millera,† María U. Alzueta,† and Rafael Bilbao†

Aragón Institute of Engineering Research, Department of Chemical and Environmental Engineering, University of Zaragoza, Campus Río Ebro, C/ María de Luna 3, 50018 Zaragoza, Spain, and Department of Mechanical Engineering, University of Zaragoza, Campus Río Ebro, C/ María de Luna 3, 50018 Zaragoza, Spain

The influence of different operation conditions (temperature, inlet acetylene concentration, and gas residence time) on the formation of soot from C_2H_2 pyrolysis has been studied. Pyrolysis experiments were carried out in a quartz reactor in the 1000−1200 °C temperature range, for different inlet C_2H_2 concentrations (15 000, 30 000, and 50 000 ppmv) and two gas residence times (1 706/*T* (K) and 4 552/*T* (K) s). Outlet gases were analyzed by gas chromatography, and the amount of soot produced was measured. The reactivity of the soot samples formed toward O_2 was also studied. The results are supported by means of different soot characterization techniques: elemental analysis, determination of Brunauer−Emmett−Teller (BET) area, transmission electron microscopy, and Raman spectroscopy. A study of the influence of these operation conditions on the resultant soot oxidative reactivities has been carried out.

1. Introduction

Soot is an important particulate pollutant in the atmosphere, and it can cause a harmful effect on the climate and health.[1] Furthermore, the amount of soot generated in a combustion system is a measure of inefficiency.[2] Therefore, the reduction of soot emissions from combustion processes is an important goal. This reduction depends both on the soot formation and its oxidation.[3]

In this context, understanding soot generation from simple hydrocarbon fuels is fundamental to establish practical strategies for increasing combustion efficiency at the same time as limiting particulate emissions.[4] The soot formation and growth in combustion systems involves a series of complex steps, following the hydrogen-abstraction−C_2H_2-addition (HACA) mechanism, a repetitive reaction sequence of two principal steps: abstraction of a hydrogen atom from the aromatic-edge C−H bond by a gaseous hydrogen atom, followed by addition of a gaseous acetylene molecule to the formed surface radical site.[5,6] The resultant soot is a mixture consisting of carbon solids and organics, such as polyaromatic hydrocarbons (PAHs).[7] Investigations on the composition and morphology of soot generated in combustion systems are of considerable importance to the understanding of physical and chemical processes of soot inception, growth, and oxidation.[8,9]

The soot reactivity is mainly determined by its composition and structure. Key physical parameters for soot are its particle size and morphology. Soot is primarily composed of carbon (>80%) and consists of agglomerated primary particles with diameters on the order of 10−30 nm comprising crystalline and amorphous domains, which form irregular clusters. The actual physical and chemical structure of soot, its elemental composition, and the ratio of crystalline graphite-like to amorphous carbon depend on the starting materials and the conditions of the combustion or pyrolysis process (fuel type, temperature, residence time, etc.).[10,11]

In this context, the present investigation seeks to contribute to a better understanding of the formation, reactivity, and structure of the soot obtained under different conditions from C_2H_2 pyrolysis, which is considered as the main soot precursor. An experimental study of acetylene pyrolysis has been undertaken modifying three operation conditions: temperature, inlet acetylene concentration, and gas residence time. In this way, the influence of these operation conditions on the resultant soot properties can be analyzed.

2. Experimental Section

2.1. Soot Formation. Experiments of C_2H_2 pyrolysis have been carried out in the facility shown in Figure 1. This setup has been used with success in previous work.[12,13] It consists of a gas-feeding system, a reaction system, a soot-collection system, and a gas-analysis system. Reaction takes place in a quartz tube reactor of 45 mm internal diameter and 800 mm length. The reactor inlet and outlet can be cooled by an air flow, which allows for controlling the temperature profile inside the reactor. Longitudinal temperature values inside the reactor have been determined by means of an S-type thermocouple in the experimental conditions considered. Additionally, the reactor outlet is mobile and can be adjusted to different positions in order to vary the gas residence time. The soot formed in the reaction is collected in quartz fiber filters of 25 mm diameter and 60 mm length, with a pore light < 1 μm.

In the experiments, a given flow rate of C_2H_2 diluted in nitrogen is fed into the reaction system, which is heated at different temperatures: 1 000, 1 050, 1 100, 1 150, and 1 200 °C. The inlet C_2H_2 concentrations used are 15 000, 30 000, and 50 000 ppmv, and the total flow rate in all experiments is 1 000 mL/min (standard temperature and pressure (STP)). As has been mentioned, the gas residence time into the reactor, defined as the reaction zone volume divided by the total gas flow rate introduced, can be varied by changing the position of the reactor cooled outlet. In this study, two gas residence times are

* Corresponding author. Phone: 0034976761150. Fax: 0034976761879. E-mail: pilruiz@unizar.es.

† Aragón Institute of Engineering Research, Department of Chemical and Environmental Engineering.

‡ Department of Mechanical Engineering.

10.1021/ie070008i CCC: $37.00
Published on Web 05/16/2007

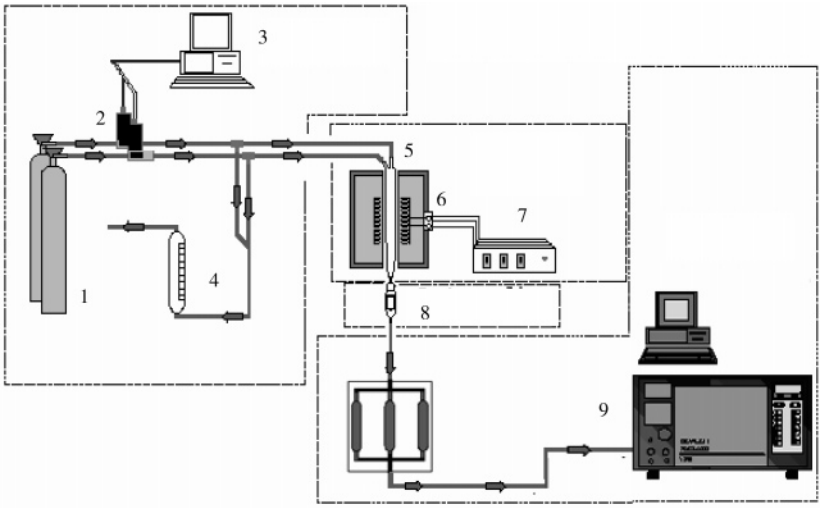

Figure 1. Experimental setup used for the C_2H_2 pyrolysis experiments: 1, N_2 and C_2H_2 cylinders; 2, mass flow meters; 3, control unit; 4, bubble flow meter; 5, quartz reactor; 6, electric furnace; 7, temperature controller; 8, soot sampling filter; and 9, gas chromatograph.

Table 1. Elemental Analysis, C/H Ratio (Molar Basis), BET Surface Area (m^2/g), Particle Sizes, and Intensity Ratio from Raman Spectra of the Soot Samples Formed under Different Conditions

soot formation experimental conditions			elemental analysiswt (%) (dry basis)							
t_r (s)	$[C_2H_2]$ (ppmv)	T (°C)	C	H	N	S	C/H (molar basis)	S_g (m^2/g)	d_p (nm)	I_g/I_d
1 706/T (K)		1 000	94.99	0.44	0.00	0.00	17.99	73.6	180−270	1.086
	15 000	1 100	97.36	0.16	0.00	0.00	50.71	40.5	80−100	1.051
		1 200	97.29	0.19	0.00	0.00	42.67	35.9	80−100	1.068
		1 000	97.72	0.43	0.00	0.00	18.94	30.4	180−250	1.041
	50 000	1 100	97.88	0.22	0.00	0.00	37.08	14.2	100−140	1.065
		1 200	98.17	0.24	0.00	0.00	34.08	15.8	80−130	1.121
4 552/T (K)		1 000	97.70	0.27	0.00	0.00	30.15	35.7	160−240	1.033
	15 000	1 100	95.75	0.15	0.00	0.00	53.19	37.2	110−130	1.057
		1 200	97.60	0.16	0.00	0.00	50.83	22.9	65−120	1.103
		1 000	97.35	0.26	0.00	0.00	31.20	11.2	140−210	1.027
	50 000	1 100	97.05	0.16	0.00	0.00	50.55	20.2	110−190	1.071
		1 200	97.79	0.12	0.00	0.00	67.91	18.2	80−120	1.093

employed, 1 706/T (K) and 4 552/T (K) s. Each experiment has been run until the necessary significant amount of soot was collected (>1 g), not exceeding a pressure limit (50 mbar) above which the functioning of the experimental setup could be disturbed. This results in an ∼3 h time experiment. In each experiment, the outlet gas composition has been analyzed by gas chromatography and the obtained soot has been quantified. The gas chromatograph allows for analyzing the following gases: H_2, CH_4, C_2H_2, C_2H_4, compounds with three (C_3) and four (C_4) carbon atoms, and C_6H_6. For further soot reactivity study and characterization analyses, and in order to eliminate the adsorbed compounds on the formed soot samples, the raw samples are annealed during 1 h in a N_2 atmosphere at 1 100 °C, except the soot samples produced at lower temperatures, which are annealed at their formation temperature to avoid possible structural changes.

2.2. Soot Reactivity. In order to study the reactivity of the soot samples formed, soot oxidation experiments have been carried out in a quartz reactor for a temperature of 1 000 °C, a total flow rate of 1 000 mL/min (STP), and an inlet O_2 concentration of 500 ppmv. Although this oxygen concentration is low for a real system, it was chosen after several tests for being low enough to allow the study of the reactivity of the soot, with a not-too-long experiment duration. With higher oxygen concentrations, the reaction is too fast and, thus, the analysis of the results obtained would lead to error.

The experimental setup used for the soot reactivity experiments is shown in Figure 2. This setup has been used in a previous work.[12] A control panel connected to mass flow controllers is used to prepare a mixture of gases (N_2/O_2) from gas cylinders. The desired mixture is directed to a quartz reactor of 550 mm length and 15 mm internal diameter.

For every experiment, the amount of soot introduced into the reactor is ∼10 mg, and it is always previously mixed with 350 mg of silica sand (150 μm). The mixture is located on a quartz wool plug placed in a bottleneck in the middle of the reactor, resulting in a thin layer. The sand is necessary to facilitate the introduction of the sample into the reactor and to prevent agglomeration of the soot particles. An inert flow of N_2 is fed while the sample is heated up to the reaction temperature (1 000 °C). Once this setpoint is reached, the reactant gas mixture is fed. The reaction temperature is measured by a thermocouple placed 0.5 cm just below the quartz wool plug where the reaction takes place. The reaction products are evacuated and then cooled down to room temperature. Prior to the analysis system, a particle filter is placed in order to retain any solid particle. The reaction products are continuously measured by Uras14/IR CO/CO_2 analyzer.

During soot oxidation, carbon is mainly lost from the particles in the form of CO and CO_2. The carbon weight in the reactor at any time can be calculated from the measured time variation of CO and CO_2 concentrations in ppm (C_{CO} and C_{CO_2}, respectively) of the exhaust gas. In this way, the total initial

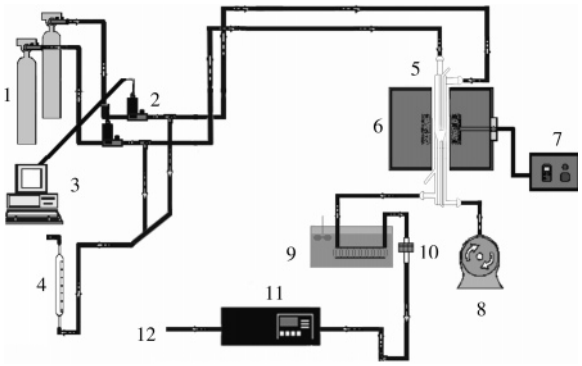

Figure 2. Experimental setup used for the soot oxidation tests: 1, N_2 and O_2 cylinders; 2, mass flow meters; 3, control unit; 4, bubble flow meter; 5, quartz reactor; 6, electric furnace; 7, temperature controller; 8: compressor; 9, condenser; 10, particle filter; 11, CO/CO_2 analyzer; and 12, vent.

amount of carbon (in mol) in the reactor, N_{C_o}, is calculated as follows,

$$N_{C_o} = F_T \times 10^{-6} \int_0^{\infty} (C_{CO} + C_{CO_2})\, dt \qquad (1)$$

where F_T is the outlet flow expressed in mol per unit time and is expressed by eq 2.

$$F_T = \frac{QP}{R_g T} \qquad (2)$$

where Q is the feeding flow rate, P is the reactor pressure, R_g is the universal gas constant in appropriate units, and T is the reactor temperature.

The amount of carbon (in mol) in the reactor at any time is calculated as follows:

$$N_C = N_{C_o} - F_T \times 10^{-6} \int_0^{t} (C_{CO} + C_{CO_2})\, dt \qquad (3)$$

Therefore, the carbon weight in the reactor at any time, W_C, is determined as

$$W_C = N_C M_C \qquad (4)$$

where M_C is the atomic weight of carbon.

In this way, the evolution of carbon conversion (X_c) as a function of time can be calculated for every experiment. The carbon conversion is defined as the amount of carbon reacted in the experiment, related to the amount of carbon fed into the reactor. The X_c values have been considered as representative values of the soot oxidative reactivities. Therefore, the oxidative reactivity of the soot samples obtained from acetylene pyrolysis under different conditions of temperature, inlet acetylene concentration, and gas residence time can be evaluated.

2.3. Soot Characterization. As has been mentioned, apart from the oxidative reactivity study, different characterization techniques are used to contribute to the knowledge of the structure and composition of the soot samples formed. These techniques are as follows: elemental analysis, determination of Brunauer−Emmett−Teller (BET) area, transmission electron microscopy (TEM), and Raman spectroscopy. The elemental analyses have been carried out in a Carlo Erba CHNS-O EA1108 analyzer. A Quantachrome AUTOSORB-6 gas adsorption analyzer is used for the surface area analyses with N_2 at 77 K. TEM images have been obtained using a JEOL JEM-2010 microscope, and for Raman analyses, a Jobyn Yvon Horiba LabRam spectrometer has been used.

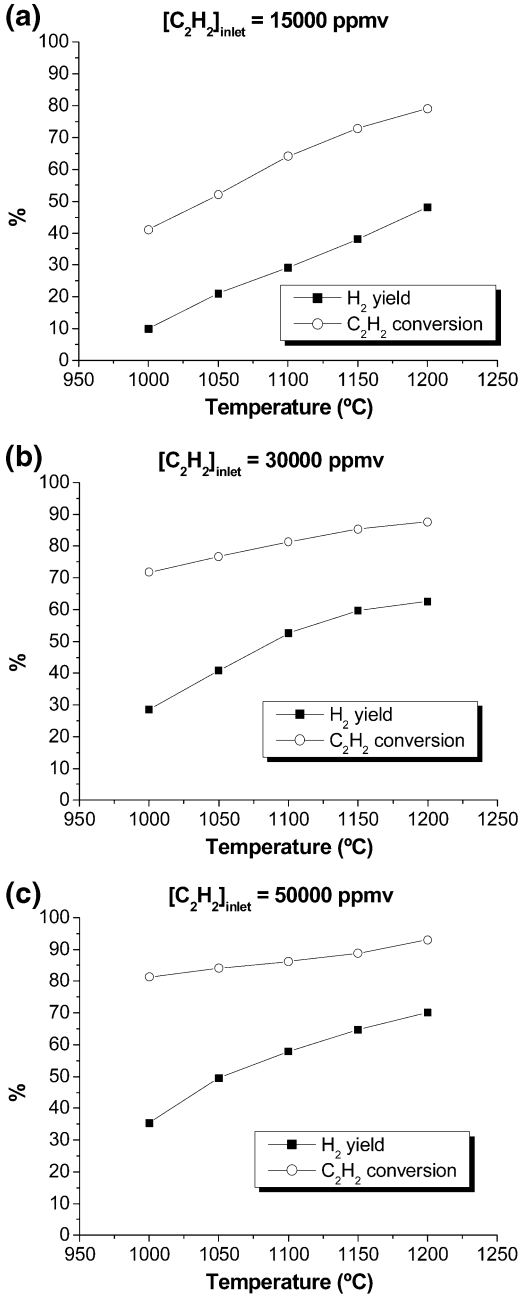

Figure 3. Evolution of H_2 yield and C_2H_2 conversion in the C_2H_2 pyrolysis experiments carried out at different temperatures, for a gas residence time of 1 706/T (K) s and three different inlet C_2H_2 concentrations: (a) 15 000 ppmv, (b) 30 000 ppmv, and (c) 50 000 ppmv.

3. Results and Discussion

The C_2H_2 pyrolysis experiments have been carried out varying temperature, inlet acetylene concentration, and gas residence time. Next, the results obtained from the influence study of these operation conditions on soot formation and its oxidative reactivity are presented.

3.1. Influence of the Pyrolysis Temperature. 3.1.1. Acetylene Pyrolysis. The effect produced by temperature is analyzed studying five different pyrolysis temperatures: 1 000, 1 050, 1 100, 1 150, and 1 200 °C. The pyrolysis experiments have been carried out with a gas residence time of 1 706/T (K) s and three different inlet acetylene concentrations (15 000, 30 000,

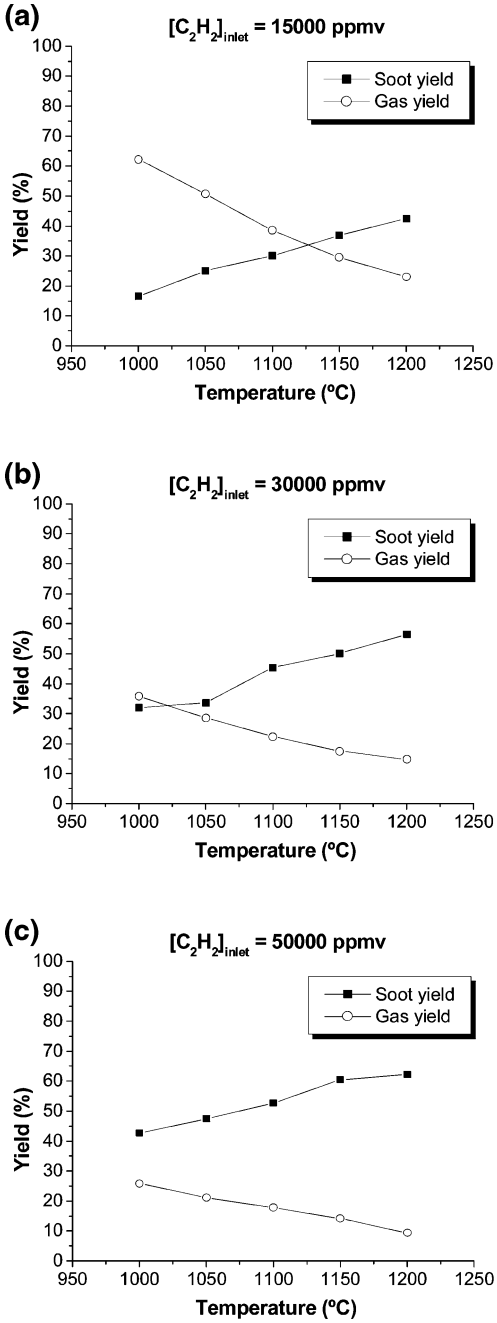

Figure 4. Soot and gas yields in the C_2H_2 pyrolysis experiments carried out at different temperatures, for a gas residence time of 1 706/*T* (K) s and three different inlet C_2H_2 concentrations: (a) 15 000 ppmv, (b) 30 000 ppmv, and (c) 50 000 ppmv.

and 50 000 ppmv). In this work, the attention has been centered in the majority gases analyzed, H_2 and C_2H_2. In all cases, the total amount (in ppmv) of the other gases analyzed (CH_4, C_2H_4, C_3, C_4, and C_6H_6) represents a percentage lower than 10% with respect to the total amount (in ppmv) of hydrogen and acetylene. The results of hydrogen yield and acetylene conversion in these experiments are shown in Figure 3. The H_2 yield is defined as the percentage of the H_2 moles produced in the experiment, related to the C_2H_2 moles introduced into the reactor. The acetylene conversion is defined as the percentage of the C_2H_2 amount reacted in the experiment, related to the C_2H_2 amount fed into the reactor. An increment of the H_2 yield and C_2H_2 conversion with the temperature has been observed, with a higher influence of the temperature for the inlet acetylene concentration of 15 000 ppmv.

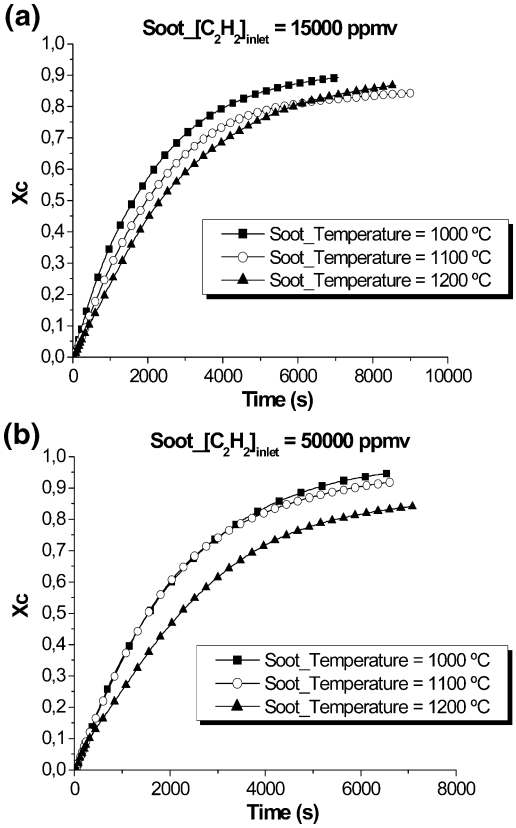

Figure 5. Evolution of the carbon conversion as function of time in the soot oxidation experiments, for the soot samples formed at different temperatures, for a gas residence time of 1 706/*T* (K) s and two different inlet C_2H_2 concentrations: (a) 15 000 ppmv and (b) 50 000 ppmv.

Furthermore, the results of soot and gas yields obtained in these experimental series are shown in Figure 4. They are defined as the percentage of the carbon amount in the soot or in the gases, related to the carbon amount introduced into the reactor. For the three inlet C_2H_2 concentrations studied, the same trend with increasing temperature is observed: an increase in soot yield and a decrease in gas yield. In all cases, the soot yield increases significantly, increasing the temperature from 1 000 to 1 200 °C. The increase of soot yield with the temperature has been previously reported in the literature.[14−16]

3.1.2. Soot Reactivity. Experiments of the interaction between some of the soot samples formed under different conditions and oxygen have been performed for an inlet oxygen concentration of 500 ppmv and for a temperature of 1 000 °C.

A comparison of the evolution of carbon conversion with time for the oxidation experiments performed with the soot samples obtained at three different temperatures is shown, as an example, in Figure 5. The results correspond to the soot oxidation experiments carried out with the soot samples obtained at 1 000, 1 100, and 1 200 °C, with a residence time of 1 706/*T* (K) s and two inlet acetylene concentrations (15 000 and 50 000 ppmv). As can be observed, in both cases, the soot samples obtained at lower temperatures are more reactive toward oxygen.

The reactivity of a material is directly related to its structure and composition.[17−20] In this study, some characterization techniques, such as elemental analysis, determination of BET area, transmission electron microscopy, and Raman spectroscopy, have been used to study the properties of the soot samples. The elemental analyses of the soot samples, as well as the C/H ratio in molar basis, are summarized in Table 1. As can be observed, all the soot samples are mainly composed by carbon

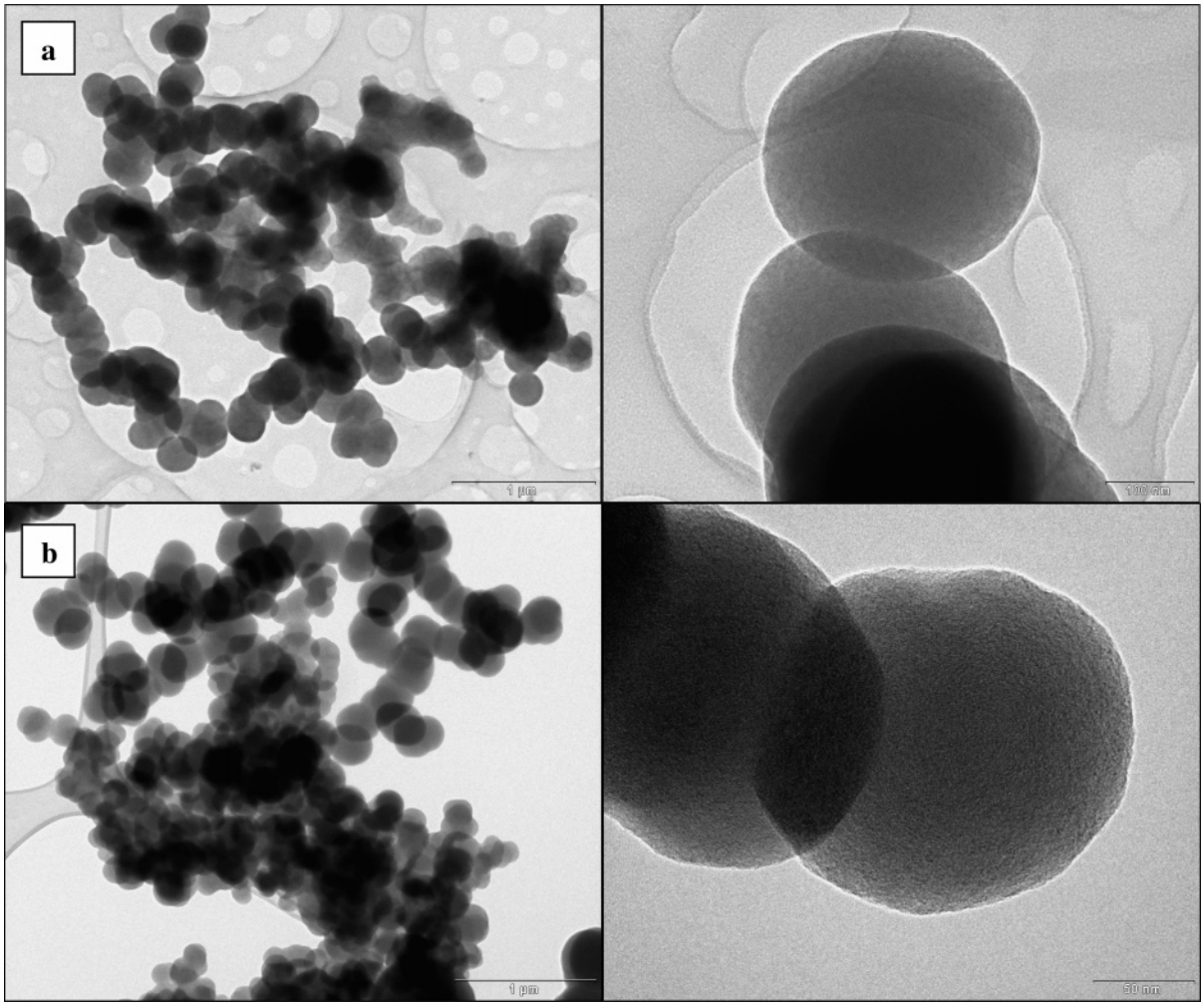

Figure 6. TEM images of the soot samples obtained under the following conditions: (a) $T = 1\,000$ °C, $[C_2H_2] = 15\,000$ ppmv, and a gas residence time of 1 706/T (K) s; (b) $T = 1\,000$ °C, $[C_2H_2] = 50\,000$ ppmv, and a gas residence time of 1 706/T (K) s.

Table 2. Values of C_2H_2 Conversion and H_2, Soot, and Gas Yields in the Acetylene Pyrolysis Experiments Carried Out at Three Different Gas Residence Times (1 706/T (K), 3 983/T (K), and 4 552/T (K) s), for Inlet Acetylene Concentrations of 15 000 and 50 000 ppmv and Three Temperatures (1 000, 1 100, and 1 200 °C)

soot formation experimental conditions						
$[C_2H_2]$ (ppmv)	T (°C)	t_r (s)	$X_{C_2H_2}$ (%)	H_2 yield (%)	soot yield (%)	gas yield (%)
15 000		1 706/T (K)	42.06	9.66	16.52	62.20
	1 000	3 983/T (K)	51.70	13.72	27.15	53.48
		4 552/T (K)	56.80	17.20	27.97	48.53
		1 706/T (K)	65.00	28.36	30.04	38.60
	1 100	3 983/T(T (	71.20	36.70	35.71	32.30
		4 552/T (K)	73.70	38.96	36.00	30.33
		1 706/T (K)	79.70	46.86	42.42	23.10
	1 200	3 983/T (K)	81.40	50.62	43.30	21.53
		4 552/T (K)	82.60	51.94	44.33	20.52
50 000	1 000	1 706/T (K)	81.40	35.13	42.56	25.84
		4 552/T (K)	87.00	44.66	50.06	21.42
	1 100	1 706/T (K)	86.20	57.59	52.66	17.77
		4 552/T (K)	89.70	62.91	58.68	14.81
	1 200	1 706/T (K)	92.30	69.73	63.47	10.32
		4 552/T (K)	93.30	75.13	63.91	9.98

(>90 wt % in all cases). Besides, the higher the soot formation temperature, the lower is the hydrogen content and, thus, the higher are the C/H ratios.

The surface area of a solid can also be related on its reactivity. The surface area values, determined by nitrogen adsorption at 77 K, for some of the soot samples formed in this work are also summarized in Table 1. The general trend is a decrease in surface area with increasing temperature. In all cases, the surface area values are significantly low, being of the same order of magnitude as their external surfaces. In order to make this assumption, the soot particles have been considered as nonmicroporous spheres, and the soot external surface has been defined as the external area of the sphere divided into the mass of the sphere. This is consistent with the fact that soot particles are nonporous or have limited porosity.[12,21,22]

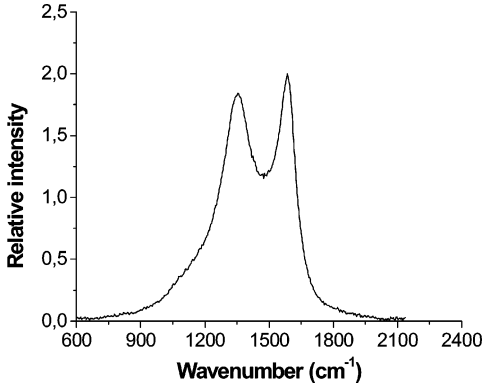

Figure 7. Raman spectrum of the soot obtained under the following conditions: $T = 1\,000$ °C, $[C_2H_2] = 15\,000$ ppmv, and a gas residence time of 1 706/T (K) s.

The soot samples have also been characterized by transmission electron microscopy. This technique is well-suited for the

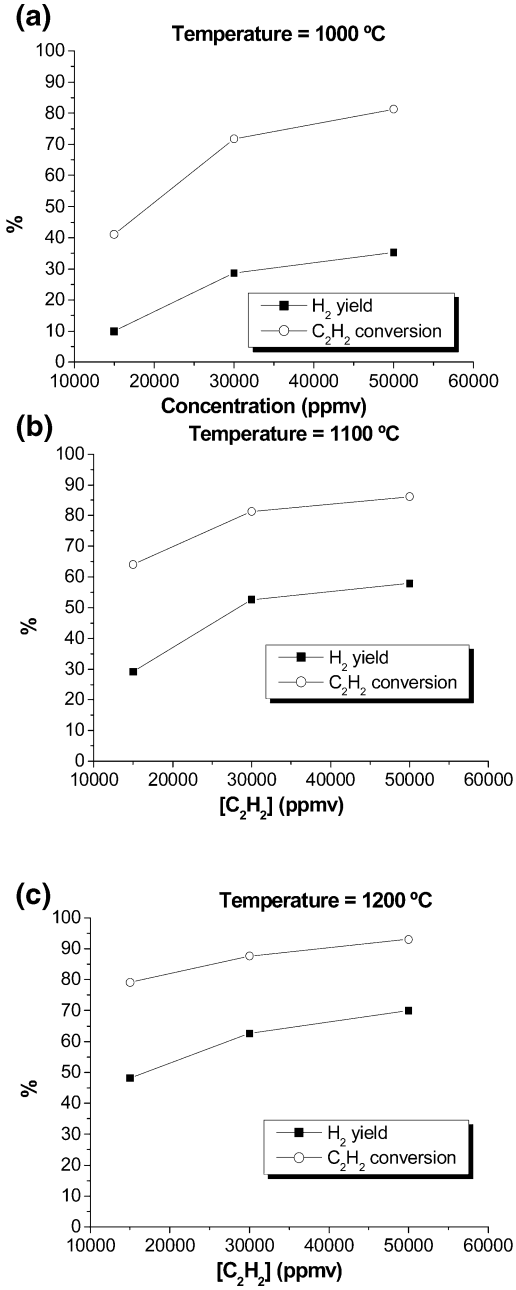

Figure 8. Evolution of H_2 yield and C_2H_2 conversion in the C_2H_2 pyrolysis experiments carried out at different inlet C_2H_2 concentrations, for a gas residence time of 1 706/*T* (K) s and three different temperatures: (a) 1 000 °C, (b) 1 100 °C, and (c) 1 200 °C.

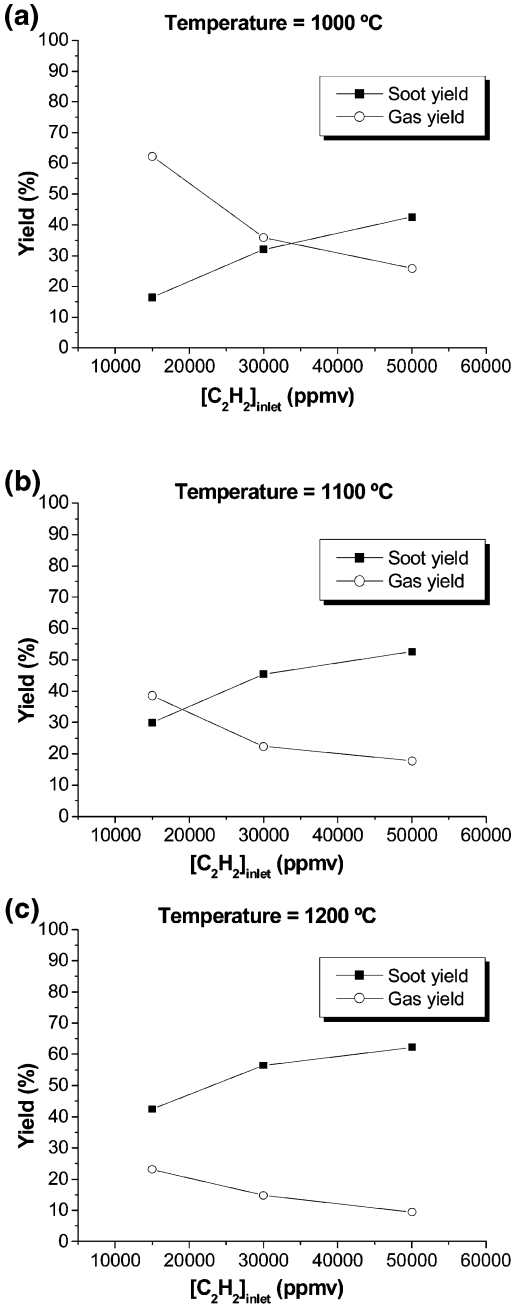

Figure 9. Soot and gas yields in the C_2H_2 pyrolysis experiments carried out at different inlet C_2H_2 concentrations, for a gas residence time of 1 706/*T* (K) s and three different temperatures: (a) 1 000 °C, (b) 1 100 °C, and (c) 1 200 °C.

morphological and chemical characterization of soot individual particles.[23−30] All the soot samples obtained in this study present a similar structure, observed by TEM. As an example, the TEM images for two samples obtained with different inlet C_2H_2 concentrations are shown in Figure 6. It can be observed that soot has the appearance of chainlike aggregates composed of several tens or hundred of subunits, known as monomers or spherules. The primary soot particles present an onionlike structure. Moreover, from TEM micrographs, it is possible to determine the soot primary particle size, which is an important structural parameter. In this study, an average size of the particles has been obtained for every soot sample. The results are shown in Table 1. A decrease in the average particle size is produced with increasing the soot-formation temperature. This phenomenon can be attributed to the shrinkage of the outer shell due to the growth and alignment of the grapheme sheets.[31−33] By increasing the temperature, the initially amorphous soot is converted to a progressively more graphitic material with some decrease in particle size.[12]

Finally, an analysis of Raman spectroscopy is carried out with the different soot samples formed. This technique has been widely used with carbon materials because an analysis of the spectra allows the inference of internal physical characteristics of the samples such as the degree of the structural disorder.[9,34−36] As an example, the Raman spectrum obtained for one of the soot samples produced is shown in Figure 7. Two peaks are observed: the D peak, centered about 1 350 cm^{-1}, and the G peak, centered about 1 590 cm^{-1}. The D peak corresponds to the disordered carbon, and the G peak corresponds to graphite. From this spectrum, by means of mathemati-

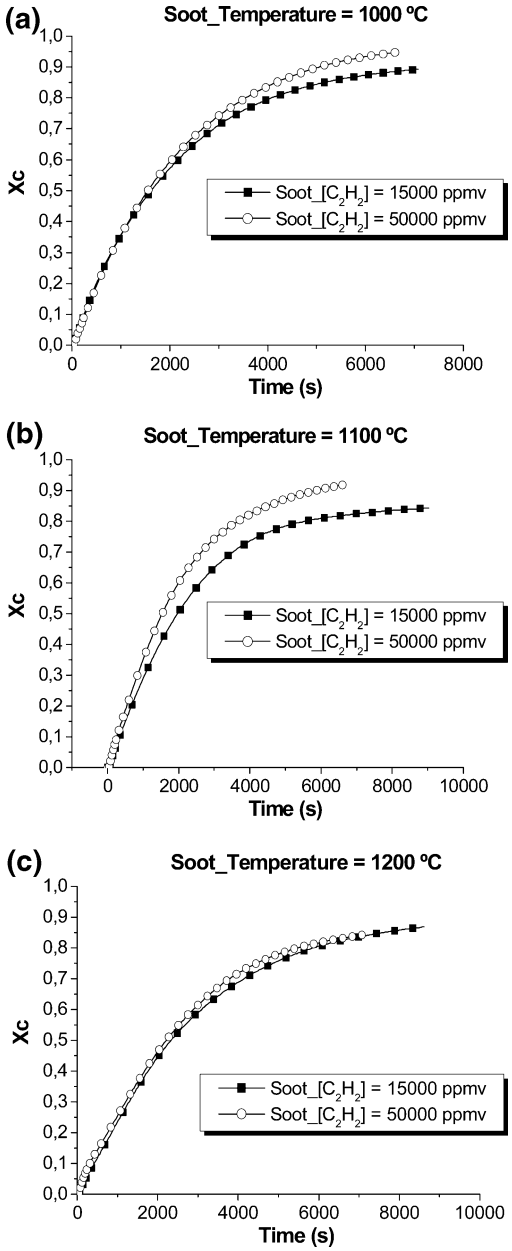

Figure 10. Evolution of the carbon conversion as a function of time in the soot oxidation experiments, for the soot samples formed at different inlet C_2H_2 concentrations, for a gas residence time of 1 706/*T* (K) s and three different temperatures: (a) 1 000 °C, (b) 1 100 °C, and (c) 1 200 °C.

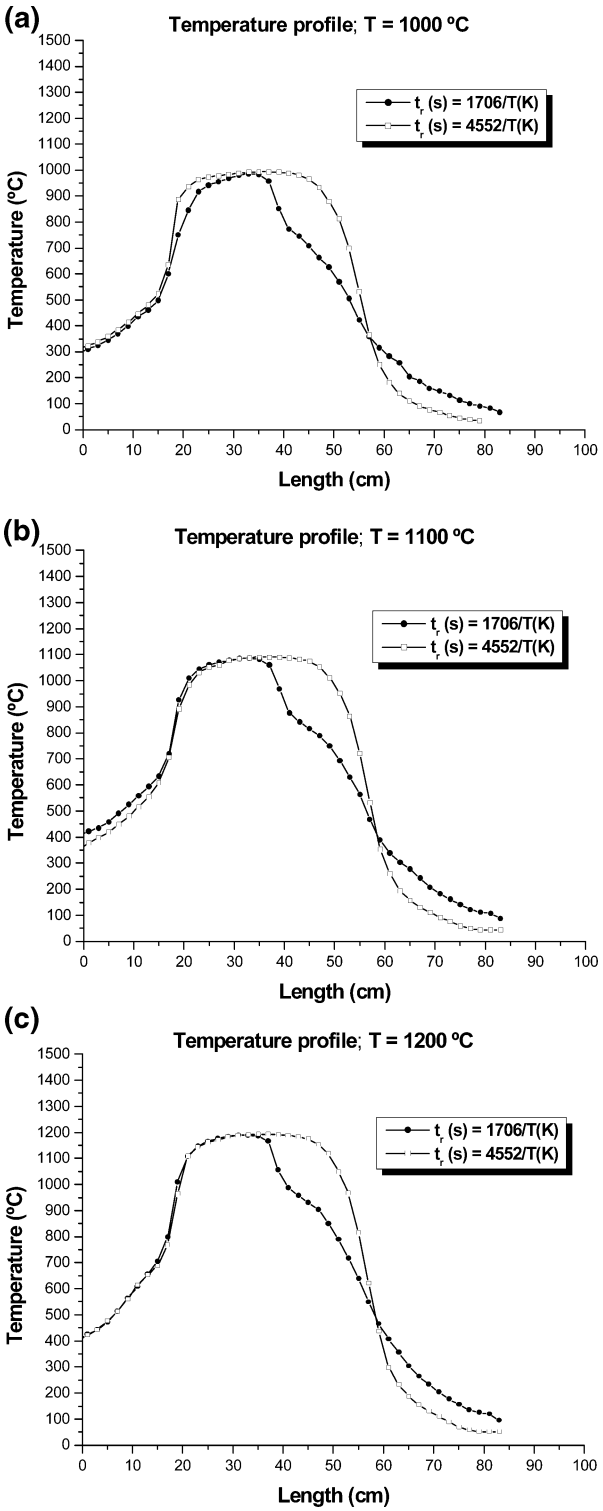

Figure 11. Temperature profile in the C_2H_2 pyrolysis reactor, for the two gas residence times employed (1 706/*T* (K) and 4 552/*T* (K) s), at different temperatures: (a) 1 000 °C, (b) 1 100 °C, and (c) 1 200 °C.

cal calculations and models, it is possible to obtain an intensity ratio between the two peaks (I_G/I_D), which is directly related to the graphitic order of the material.[12] In this way, the intensity ratios for the different soot samples can be calculated (Table 1). In general, for the different experimental series analyzed, an increase in formation temperature leads to an increase in the graphitic order of the soot. This graphitization process that occurs at higher temperatures has been previously reported in the literature.[37,38]

Consequently, it has been observed that the soot samples obtained at higher temperatures are less reactive toward oxygen. This behavior can be justified by higher C/H ratios and a more ordered structure of the soot samples obtained at higher temperatures.

3.2. Influence of the Pyrolysis Initial Acetylene Concentration. 3.2.1. Acetylene Pyrolysis. In the study of the influence of the inlet acetylene concentration, three acetylene concentrations are used: 15 000, 30 000, and 50 000 ppmv. In Figure 8, one can see the results of hydrogen yield and acetylene conversion corresponding to the experiments carried out with a gas residence time of 1 706/*T* (K) s and three temperatures: 1 000, 1 100, and 1 200 °C . As can be observed, both of them increase with acetylene concentration, reaching high acetylene conversions (>90%) for the initial acetylene concentration of 50 000 ppmv. With respect to soot and gas yields, Figure 9 shows that an increase in the acetylene concentration leads to

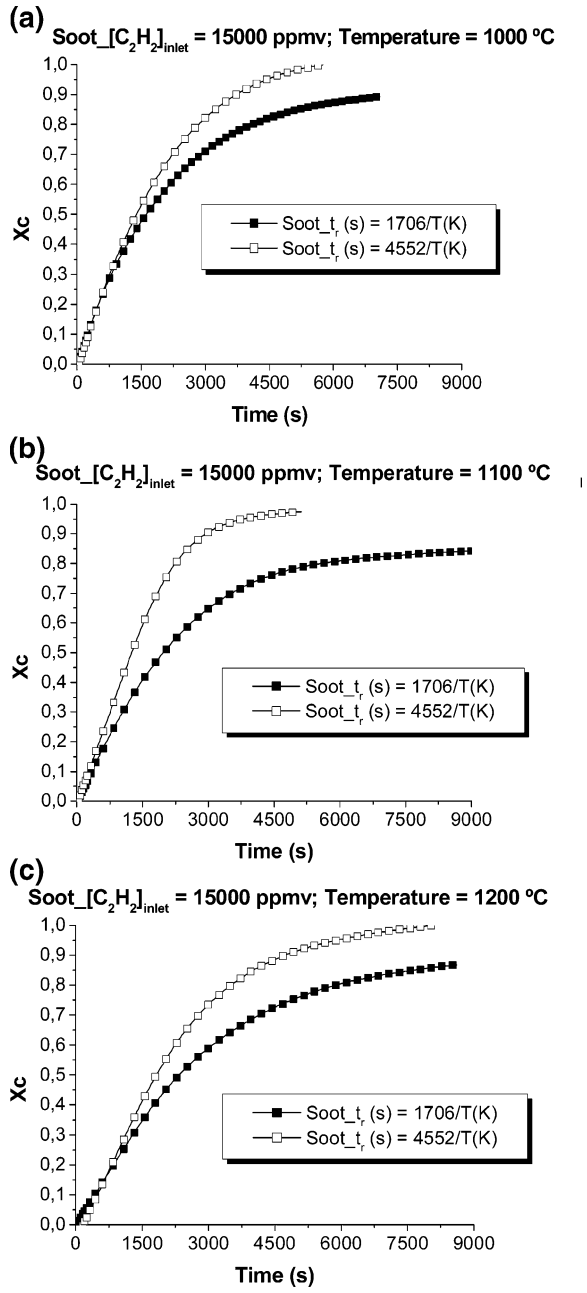

Figure 12. Evolution of the carbon conversion as a function of time in the soot oxidation experiments, for the soot samples formed at two different gas residence times (1 706/*T* (K) and 4 552/*T* (K) s), for an inlet C_2H_2 concentration of 15 000 ppmv and three different temperatures: (a) 1 000 °C, (b) 1 100 °C, and (c) 1 200 °C.

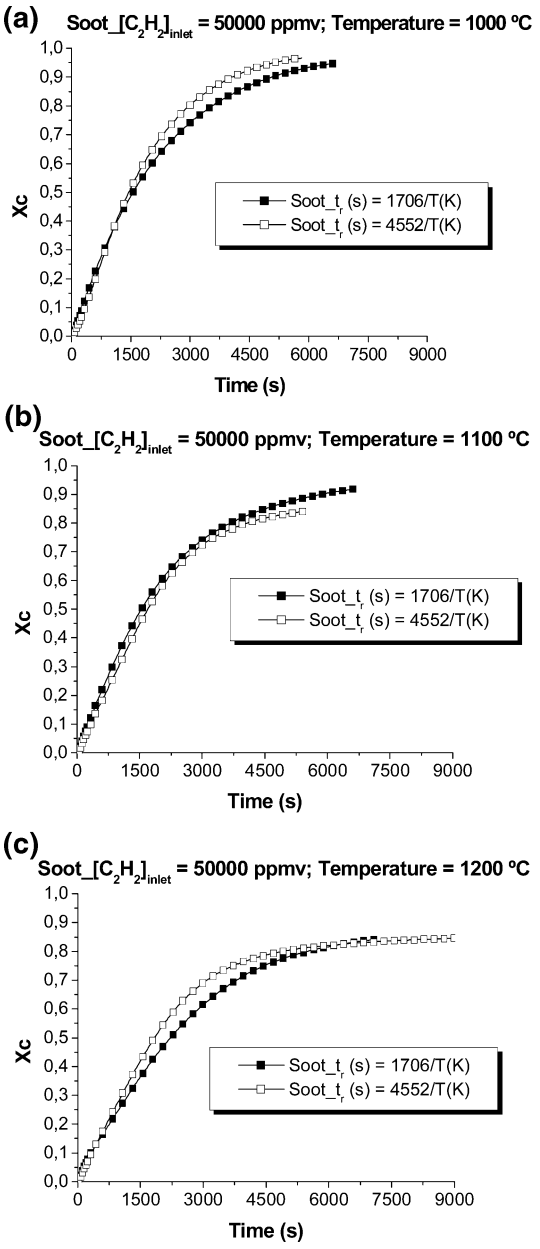

Figure 13. Evolution of the carbon conversion as a function of time in the soot oxidation experiments, for the soot samples formed at two different gas residence times (1 706/*T* (K) and 4 552/*T* (K) s), for an inlet C_2H_2 concentration of 50 000 ppmv and three different temperatures: (a) 1 000 °C, (b) 1 100 °C, and (c) 1 200 °C.

an increase in soot yield and a decrease in gas yield, with a more significant influence of the inlet C_2H_2 concentration at lower temperatures.

3.2.2. Soot Reactivity. The effect of pyrolysis inlet acetylene concentration in the further soot oxidative reactivity has also been studied. The evolution of carbon conversion as a function of time, for the soot samples obtained at two different inlet acetylene concentrations, is shown in Figure 10. As can be noted, the carbon materials formed with an acetylene concentration of 50 000 ppmv are slightly more reactive toward oxygen than the soot samples produced with 15 000 ppmv of acetylene, with the differences being higher at lower temperatures. In this case, neither soot elemental analysis nor particle size nor Raman intensity ratio (Table 1) show a clear dependence with pyrolysis inlet acetylene concentration. As can be observed in the TEM images in Figure 6, the soot samples obtained with 50 000 ppmv of acetylene are more aggregated than the samples obtained with 15 000 ppmv of acetylene, and thus, they could have more carbon in junction sites available to react. Since a carbon atom at an edge or junction site is more reactive than one in the basal plane of a grapheme layer, a soot with many populated edge or junction sites has a higher reactivity.[39,40] This may be a reason for the soot samples produced with higher acetylene concentrations to be more reactive toward oxygen. This aggregation could also explain the decrease in surface area observed with increasing the inlet acetylene concentration (Table 1). As has been mentioned above, the soot particles are nonporous materials, with their surface area being of the same order of magnitude as their external area.

3.3. Influence of the Gas Residence Time. 3.3.1. Acetylene Pyrolysis. Two different gas residence times have been used in this work, 1 706/*T* (K) and 4 552/*T* (K) s. As has been

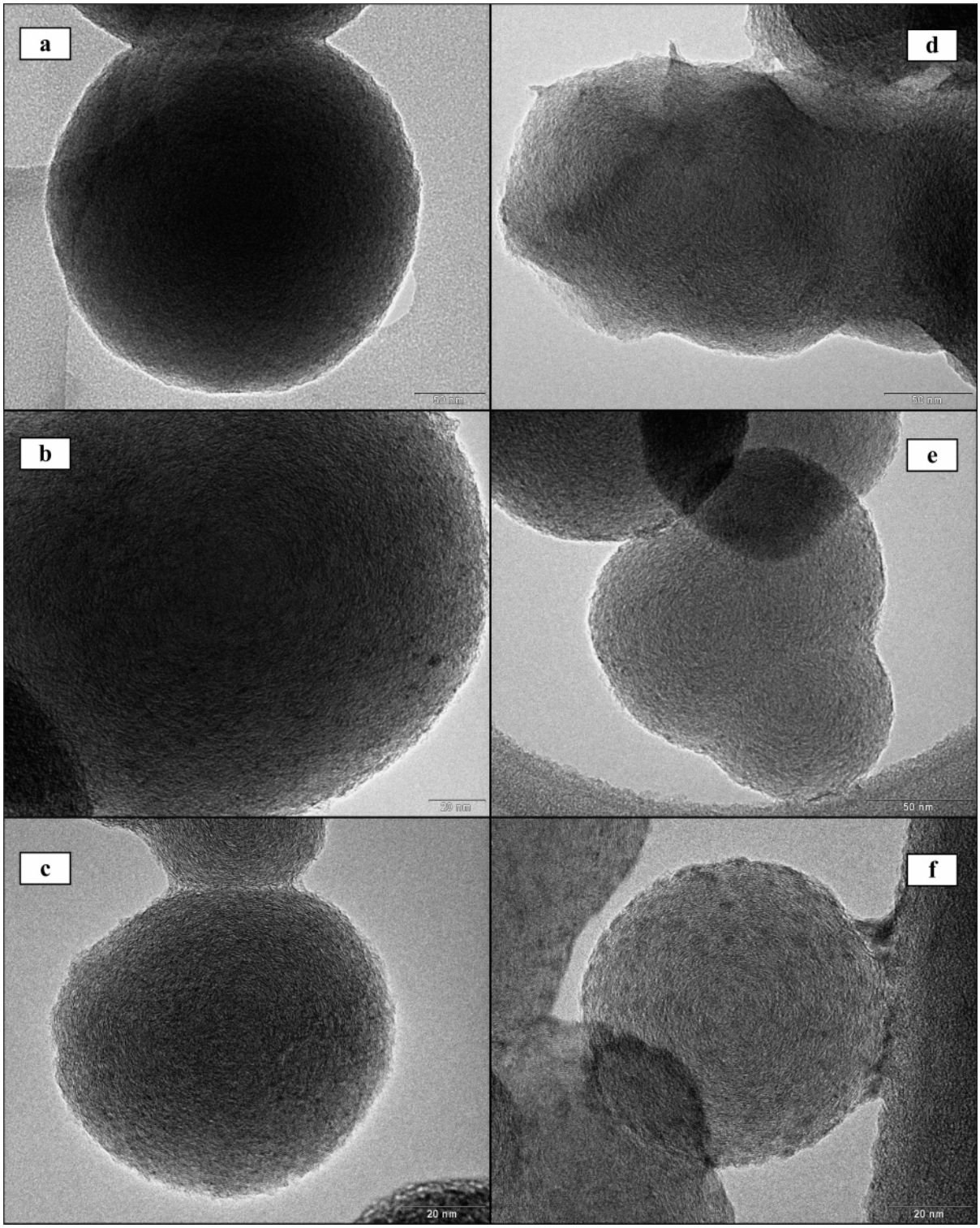

Figure 14. TEM images of the soot samples obtained at 15 000 ppmv acetylene concentration and two different gas residence times and temperatures: (a) t_r (s) = 1 706/T (K) and T = 1 000 °C; (b) t_r (s) = 1 706/T (K) and T = 1 100 °C; (c) t_r (s) = 1 706/T (K) and T = 1 200 °C; (d) t_r (s) = 4 552/T (K) and T = 1 000 °C; (e) t_r (s) = 4 552/T (K) and T = 1 100 °C; and (f) t_r (s) = 4 552/T (K) and T = 1 200 °C.

previously mentioned, these gas residence times correspond to two different positions of the reactor cooled outlet (reaction zone lengths of 6 and 16 cm, respectively, with a flat temperature profile ±25 °C) and, therefore, to two different temperature profiles inside the reactor. These temperature profiles, obtained for different setpoint temperatures of the electrical furnace, are shown in Figure 11. The results of hydrogen yield and acetylene conversion for the experiments carried out with 15 000 and 50 000 ppmv of acetylene, at three temperatures (1 000, 1 100, and 1 200 °C) and with the two gas residence times mentioned above, are shown in Table 2. In this table, the results obtained in a previous work for a gas residence time of 3 983/T (K) s and 15 000 ppmv of inlet acetylene have been also included for clarifying the trends.[12] As can be expected, H_2 yield and acetylene conversion increase with gas residence time. The corresponding results of

soot and gas yields are also presented in Table 2. An increase in gas residence time involves an increase in soot yield and a decrease in gas yield. The effect of gas residence time is higher for the experiments performed at lower temperatures and lower inlet acetylene concentrations.

3.3.2. Soot Reactivity. The evolution of carbon conversion as a function of time for the oxidation experiments, performed with the soot samples produced with different gas residence times and different inlet C_2H_2 concentrations, is shown in Figures 12 and 13. In both cases, it has been noted that the soot samples formed with higher gas residence time present higher oxidative reactivities. The trend is clearer for the experimental series made with the soot samples formed with the lowest pyrolysis inlet acetylene concentration (15 000 ppmv). As can be observed in characterization results (Table 1), the pyrolysis gas residence time does not have a clear effect on the soot properties that could explain the differences in reactivity observed.

This increase in soot reactivity with gas residence time could be attributed to a higher heterogeneity of the soot samples. Since the gas residence time in pyrolysis experiments is varied by adjusting the reactor cooled outlet at different positions, the highest gas residence time studied (4 552/T (K) s) corresponds to a wider temperature profile than the one corresponding to the lowest gas residence time (1 706/T (K) s) (Figure 11). For the lowest gas residence time, the reactant mixture (acetylene in nitrogen) reaches up the desired temperature and is immediately cooled down to low temperatures, at which soot formation is not produced. It is worth noting that, under the conditions studied, no soot formation has been observed below 1 000 °C. However, for the highest residence time, the reactor cooled outlet is outside the oven, and thus, the reactant mixture, after reacting, is slowly cooled. In this case, the temperature decay occurs progressively. Therefore, because of a wider temperature profile in the pyrolysis experiments, the soot obtained with the highest gas residence time is, in fact, a mixture of soot samples formed at different temperatures, not only at the desired one, but also at lower temperatures. As has been mentioned, these soot particles formed at lower temperatures are more reactive. This idea of higher heterogeneity of the soot samples obtained at the highest gas residence time is also supported by the TEM images shown in Figure 14. As can be observed, the primary particles of the soot samples obtained for the lowest gas residence time present a more homogeneous structure than the soot particles corresponding to the highest gas residence time.

4. Conclusions

A study of the influence of different operation conditions (i.e., temperature, initial acetylene concentration, and gas residence time) on the formation of soot from acetylene pyrolysis has been carried out. An increase in pyrolysis temperature leads to an increase in acetylene conversion and soot yield, and the soot obtained is less reactive toward oxygen, because this soot is more aromatic and graphitic. By increasing the inlet acetylene concentration, the acetylene conversion and soot yield increase and the soot produced is more reactive. This may be attributed to a higher amount of carbon in junction sites due to a higher aggregation of the soot particles. Finally, in the influence study of the gas residence time, the acetylene conversion and soot yield increase with gas residence time, and the soot samples formed at a higher gas residence time are more reactive because of the heterogeneity of the material, with the presence of soot particles formed at lower temperatures than the desired one, produced by a wider temperature profile in pyrolysis experiments.

Acknowledgment

The authors express their gratitude to the MCYT (Project PPQ2003-02394) and DGA (Project PIP104/2005) for financial support. M.P.R. acknowledges the Spanish Ministry of Science and Education (MEC) for the award of a Predoctoral Grant (BES-2005-6898).

Literature Cited

(1) Kim, W.; Sorensen, C. M.; Fry, D.; Chakrabarti, A. Soot aggregates, superaggregates and gel-like networks in laminar diffusion flames. *J. Aerosol Sci.* **2006**, *37*, 386.

(2) Klusek, C.; Manickavasagam, S.; Mengüç, M. P. Compendium of scattering matrix element profiles for soot agglomerates. *J. Quant. Spectrosc. Radiat. Transfer* **2003**, *79*−*80*, 839.

(3) Crua, C.; Kennaird, D. A.; Heikal, M. R. Laser-induced incandescence study of diesel soot formation in a rapid compression machine at elevated pressures. *Combust. Flame* **2003**, *135*, 475.

(4) Gardner, C.; Greaves, G. N.; Hargrave, G. K.; Jarvis, S.; Wildman, P.; Meneau, F.; Bras, W.; Thomas, G. In situ measurements of soot formation in simple flames using small angle X-ray scattering. *Nucl. Instrum. Methods Phys. Res., Sect. B* **2005**, *238*, 334.

(5) Frenklach, M.; Wang, H. *Soot formation in combustion: Mechanisms and models*; Bockhorn, H., Ed.; Springer: Berlin, 1994; p 165.

(6) Frenklach, M. Reaction mechanism of soot formation in flames. *Phys. Chem. Chem. Phys.* **2002**, *4*, 2028.

(7) Luo, C. H.; Grace Lee, W. M.; Lai, Y. C.; Wen, C. Y.; Liaw, J. J. Measuring the fractal dimension of diesel soot agglomerates by fractional Brownian motion processor. *Atmos. Environ.* **2005**, *39*, 3565.

(8) Tian, K.; Liu, F.; Thomson, K. A.; Snelling, D. R.; Smallwood, G. J.; Wang, D. Distribution of the number of primary particles of soot aggregates in a nonpremixed laminar flame. *Combust. Flame* **2004**, *138*, 195.

(9) Tian, K.; Thomson, K. A.; Liu, F.; Snelling, D. R.; Smallwood, G. J.; Wang, D. Determination of the morphology of soot aggregates using the relative optical density method for the analysis of TEM images. *Combust. Flame* **2006**, *144*, 782.

(10) Sadezky, A.; Muckenhuber, H.; Grothe, H.; Niessner, R.; Pöschl, U. Raman microspectroscopy of soot and related carbonaceous materials: spectral analysis and structural information. *Carbon* **2005**, *43*, 1731.

(11) Dippel, B.; Heintzenberg, J. Soot characterization in atmospheric particles from different sources by NIR FT Raman spectroscopy. *J. Aerosol Sci.* **1999**, *30* (Suppl. 1), 907.

(12) Ruiz, M. P.; Guzmán de Villoria, R.; Millera, A.; Alzueta, M. U.; Bilbao, R. Influence of the temperature on the properties of the soot formed from C_2H_2 pyrolysis. *Chem. Eng. J.* **2007**, *127*, 1.

(13) Ruiz, M. P.; Callejas, A.; Millera, A.; Alzueta, M. U.; Bilbao, R. Soot formation from C_2H_2 and C_2H_4 pyrolysis at different temperatures. *J. Anal. Appl. Pyrolysis* **2007**, *79*, 244.

(14) Alexiou, A.; Williams, A. Soot formation in shock-tube pyrolysis of toluene−*n*-heptane and toluene−iso-octane mixtures. *Fuel* **1995**, *74*, 153.

(15) Alexiou, A.; Williams, A. Soot formation in shock-tube pyrolysis of toluene, toluene−methanol, toluene−ethanol, and toluene−oxygen mixtures. *Combust. Flame* **1996**, *104*, 51.

(16) Fletcher, T. H.; Ma, J.; Rigby, J. R.; Brown, A. L.; Webb, B. W. Soot in coal combustion systems. *Prog. Energy Combust. Sci.* **1997**, *23*, 283.

(17) Vander Wal, R. L.; Tomasek, A. J. Soot nanostructure: Dependence upon synthesis conditions. *Combust. Flame* **2004**, *136*, 129.

(18) Murr, L. E.; Soto, K. F. A TEM study of soot, carbon nanotubes, and related fullerene nanopolyhedra in common fuel-gas combustion sources. *Mater. Charact.* **2005**, *55*, 50.

(19) Grieco, W. J.; Howard, J. B.; Rainey, L. C.; Vander Sande, J. B. Fullerenic carbon in combustion-generated soot. *Carbon* **2000**, *38*, 597.

(20) Werner, H.; Herein, D.; Blöcher, J.; Henschke, B.; Tegtmeyer, U.; Schedel-Niedrig, Th.; Keil, M.; Bradhaw, A. M.; Schlögl, R. Spectroscopic and chemical characterisation of "fullerene black". *Chem. Phys. Lett.* **1992**, *194*, 62.

(21) Akhter, M. S.; Chughtai, A. R.; Smith, D. M. The structure of hexane soot. I: Spectroscopic studies. *Appl. Spectrosc.* **1985**, *39*, 143.

(22) Burtscher, H.; Kuenzel, S.; Hueglin, C. Structure of particles in combustion engine exhaust. *J. Aerosol Sci.* **1995**, *26*, 129.

(23) Liu, F.; Smallwood, G. J.; Snelling, D. R. Effects of primary particle diameter and aggregate size distribution on the temperature of soot particles heated by pulsed lasers. *J. Quant. Spectrosc. Radiat. Transfer* **2005**, *93*, 301.

(24) Kis, V. K.; Pósfai, M.; Lábár, J. L. Nanostructure of atmospheric soot particles. *Atmos. Environ.* **2006**, *40*, 5533.

(25) Lapuerta, M.; Ballesteros, R.; Martos, F. J. A method to determine the fractal dimension of diesel soot aggregates. *J. Colloid Interface Sci.* **2006**, *303*, 149.

(26) Jäger, Ch.; Henning, T.; Schlögl, R.; Spillecke, O. Spectral properties of carbon black. *J. Non-Cryst. Solids* **1999**, *258*, 161.

(27) Di Stasio, S. Electron microscopy evidence of aggregation under three different size scales for soot nanoparticles in flames. *Carbon* **2001**, *39*, 109.

(28) Dobbins, R. A.; Fletcher, R. A.; Chang, H. C. The evolution of soot precursor particles in a diffusion flame. *Combust. Flame* **1998**, *115*, 285.

(29) Sgro, L. A.; Baseile, G.; Barone, A. C.; D'Anna, A.; Minutolo, A.; Borghese, A.; D'Alessio, A. Detection of combustion formed nanoparticles. *Chemosphere* **2003**, *51*, 1079.

(30) Barone, A. C.; D'Alessio, A.; D'Anna, A. Morphological characterization of the early process of soot formation by atomic force microscopy. *Combust. Flame* **2003**, *132*, 181.

(31) Kim, Y. A.; Hayashi, T.; Osawa, K.; Dresselhaus, M. S.; Endo, M. Annealing effect on disordered multi-wall carbon nanotubes. *Chem. Phys. Lett.* **2003**, *380*, 319.

(32) Richter, H.; Howard, J. B. Formation of polycyclic aromatic hydrocarbons and their growth to soot—A review of chemical reaction pathways. *Prog. Energy Combust. Sci.* **2000**, *26*, 565.

(33) Ci, L.; Zhu, H.; Wei, B.; Xu, C.; Liang, J.; Wu, D. Graphitization behaviour of carbon nanofibers prepared by the floating catalyst method. *Mater. Lett.* **2000**, *43*, 291.

(34) Guzmán de Villoria, R.; Miravete, A.; Cuartero, J.; Chiminelly, A.; Tolosana, N. Mechanical properties of SWNT/epoxy composites using two different curing cycles. *Composites Part B—Engineering* **2006**, *37*, 273.

(35) Roubin, P.; Martin, C.; Arnas, C.; Colomban, Ph.; Pégourié, B.; Brosset, C. Raman spectroscopy and X-ray diffraction studies of some deposited carbon layers in Tore Supra. *J. Nucl. Mater.* **2005**, 337−339, 990.

(36) Escribano, R.; Sloan, J. J.; Siddique, N.; Sze, N.; Dudev, T. Raman spectroscopy of carbon-containing particles. *Vib. Spectrosc.* **2001**, *26*, 179.

(37) Stanmore, B. R.; Brilhac, J. F.; Gilot, P. The oxidation of soot: A review of experiments, mechanisms and models. *Carbon* **2001**, *39*, 2247.

(38) Fernandes, M. B.; Skjemstad, J. O.; Johnson, B. B.; Wells, J. D.; Brooks, P. Characterization of carbonaceous combustion residues. I. Morphological, elemental and spectroscopic features. *Chemosphere* **2003**, *51*, 785.

(39) Song, J.; Alam, M.; Boehman, A. L.; Kim, U. Examination of the oxidation behaviour of biodiesel soot. *Combust. Flame* **2006**, *146*, 589.

(40) Vander Wal, R. L.; Tomasek, A. J. Soot oxidation: Dependence upon initial nanostructure. *Combust. Flame* **2003**, *134*, 1.

Received for review January 3, 2007
Revised manuscript received April 11, 2007
Accepted April 13, 2007

IE070008I